ELSEVIER

Surface Science 370 (1997) 268–276

surface science

Temperature-dependent surface X-ray diffraction on K/Ag(001)-(2 × 1)

H.L. Meyerheim [a,*], I.K. Robinson [b], R. Schuster [b]

[a] *Institut für Kristallographie & Angewandte Mineralogie der Universität München, Theresienstraße 41, 80333 München, Germany*
[b] *Department of Physics, University of Illinois, Urbana, IL 61801, USA*

Received 13 May 1996; accepted for publication 26 July 1996

Abstract

Temperature-dependent surface X-ray diffraction experiments have been performed on the K/Ag(001)-(2 × 1) adsorption system. The structure is characterized by a missing-row geometry in which alternate Ag rows along [1$\bar{1}$0] are missing. The K atoms reside within the large grooves coordinated by six Ag atoms at a distance of 3.44(5) Å, corresponding to an effective K-radius of 2.00(5) Å. Large anisotropic disorder is observed for both the K-atoms and the top-layer ("ridge") Ag atoms. The K-atom displacements are largest in the direction along the grooves, whereas for the Ag atoms the vibrations along [110] are significantly larger. The temperature dependence of the Ag vibrations is in accordance with Debye theory for the [110] direction, but deviates from it for the [1$\bar{1}$0] vibrations at high temperature. In contrast to the K-atoms, the out-of-plane vibrations of the top-layer Ag atoms are larger than the in-plane vibrations. The inclusion of anharmonic contributions to describe the Ag disorder significantly improves the fits. It is shown that if anharmonicity is neglected the interlayer contraction is overestimated ($\Delta d_{12}/d_{12}$ only −3.2%, instead of −12.7% if anharmonicity is neglected). Due to the anharmonicity, different definitions of the atomic position arise (mean, mode and equilibrium position), which are discussed on the basis of the results.

Keywords: Alkali metals; Anharmonic vibrations; Surface reconstruction; Surface structure; X-ray diffraction

1. Introduction

It is well known that alkali metals (AM) like K and Cs induce reconstructions on a number of low-index metal surfaces, and most interest has been focused on the (110) surfaces of fcc metal surfaces such as Ni, Cu, Ag and Pd [1–6]. For these reconstructions a missing-row (MR) geometry has been proposed, and theoretical studies of AM adsorption on fcc (110) surfaces have suggested that the more open MR structure is associated with a higher chemisorption energy for the large K atoms, because of the higher coordination of K atoms [7].

Several AM-induced reconstructions have also been reported for the fcc (001) surfaces of Ag and Cu [8–10]. For K-adsorption on Ag(001) at room temperature, Okada et al. [8,9] reported a (2 × 1) reconstruction between 0.1 and 0.2 ML coverage and a (3 × 1) reconstruction above about 0.25 ML. The absolute coverage Θ is defined as the ratio of the number density of the K atoms relative to the (unreconstructed) Ag(001) surface atoms (1 ML = 1.2×10^{15} atoms cm^{-2}). Although MR geometries have been suggested for the (2 × 1) and the (3 × 1) reconstructions and are also assumed in theoretical

*Corresponding author. Fax: +49 89 23944334; e-mail: uk40104@sunmail.lrz-muenchen.de

PII S0039-6028(96)00970-3

calculations [11], the detailed surface structure has not as yet been measured. Our surface X-ray diffraction (SXRD) structure analysis gives direct evidence for an MR-type geometry of the (2×1) reconstruction on the Ag(001) surface, and the K adsorption site within the grooves of the MR structure, confirming the principle of coordination maximization.

A complete description of the surface structure requires proper consideration of the structural disorder, which includes thermal vibrations and other displacements of the atoms. In SXRD this is generally taken into account using the harmonic model, i.e. by a Gaussian probability density function (PDF) of the atoms [12]. Little work has been done on the analysis of anharmonic vibrations, although these are expected to be even more important at the surface than in the bulk. For example, enhanced anharmonicity on surfaces has been observed by surface-extended X-ray absorption fine structure (SEXAFS) measurements and by energy-resolved He scattering data [13,14]. On the other hand, well-established long-range order techniques such as low-energy electron diffraction (LEED) and SXRD [15,16] mostly use the harmonic approximation with either isotropic or anisotropic displacements. On the basis of the present investigation on the (2×1) reconstruction, we demonstrate the importance of anharmonic thermal vibrations for the structure analysis of surfaces, as well as their possible implications on the structural parameters.

2. Experiment

The Ag(001) surface was prepared by repeated cycles of Ar^+ ion sputtering (500 eV) and annealing at about 800 K. The K atoms were deposited from thoroughly outgassed SAES dispensers. Within the sensitivity of the Auger electron spectrometer (AES) system, no traces of contaminants could be detected after deposition. The X-ray scattering experiments were performed at the beamline X16A of the National Synchrotron Light Source (NSLS) in Brookhaven (New York, USA) using the UHV diffractometer described by Fuoss et al. [17]. In-situ monitoring of half- and third-order superlattice reflections during K deposition allowed the homogeneous preparation of the (2×1) reconstruction over the sample surface, thereby avoiding the simultaneous presence of several reconstructions within the coverage regime between about $\Theta=0.18$ and 0.25 ML [8]. High-quality superstructures could be prepared in this way. From the measured width of the superlattice reflections, a correlation length of about 800 Å was determined.

After preparing the reconstruction at 330 K, the sample was cooled immediately. The XRD experiments reported here were performed at about 166, 170, 210 and 313 K. At 210 K a larger data set was taken in which 110 reflections were measured, which gave 39 symmetry-independent reflections. The data set included 16 symmetry-independent in-plane reflections and four superlattice rods measured up to 3.0 $Å^{-1}$, corresponding to a maximum out-of-plane momentum transfer of 1.95 reciprocal lattice units. Along each rod, six equidistant sampling points were generally measured. Systematic errors were estimated by the reproducibility of symmetry-equivalent reflections, which were in agreement to below 10% in most cases. The stability of the surface structure was controlled by frequent monitoring of several reflections during data collection.

3. Results and discussion

Fig. 1 shows top and side views of the structural model of the (2×1) reconstruction. Small hatched and open circles represent top- and second-layer Ag atoms (labeled $Ag_{(1)}$ and $Ag_{(2)}$ and the K atoms are indicated by large open circles. Taking account of deeper-lying Ag layers did not lead to better fits with the data.

The basic feature of the K/Ag(001)-(2×1) reconstruction is the missing-row (MR) geometry, where every other Ag chain along $[1\bar{1}0]$ is missing [18]. This is directly evident from the (projected) Patterson function as discussed in Ref. [19]. One (2×1) unit cell is indicated by the dashed rectangle shown in the upper right part of Fig. 1. Since the K coverage is only about 0.15 ML (i.e. 0.30 K atoms per (2×1) unit cell), K atoms are shown statistically to occupy 30% of the (2×1) unit cells,

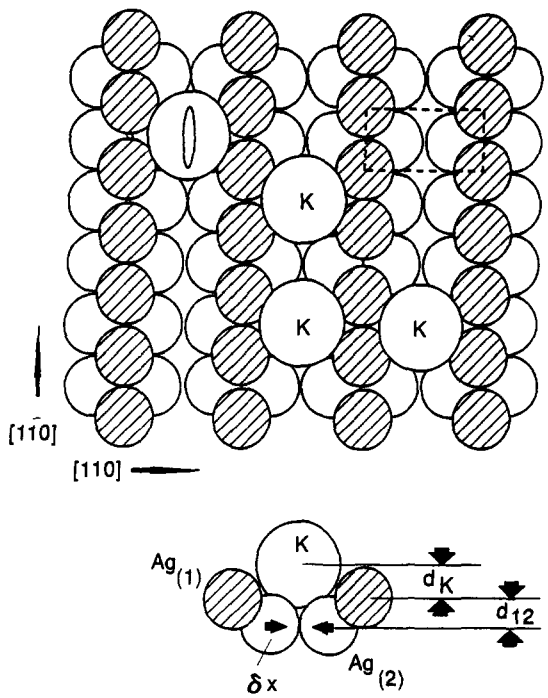

Fig. 1. Schematic drawing of the K/Ag(001)-(2 × 1) reconstruction in top and side view. Top- and second-layer Ag atoms ($Ag_{(1)}$, $Ag_{(2)}$) are shown by small hatched and open circles, respectively. Large circles represent K atoms. The ellipse in the upper left part of the figure indicates the anisotropy of the in-plane root mean square displacement of the K atoms within the rows. The (2 × 1) unit cell is indicated by the dashed rectangle ($a_0 = 5.78$ Å, $b_0 = 2.89$ Å).

thereby leaving 70% of the surface unit-cells empty. Since the X-ray diffraction technique provides a space (and time) average of the structure, a 30% statistical K-occupancy of the unit cells is equivalent to a 30% occupation probability of all (2 × 1) unit cells (coherent averaging).

The K atoms are located in the centers of the (2 × 1) unit cells and are six-fold coordinated by Ag atoms of the first and second layer. In addition, we observe for both K atoms and top-layer Ag atoms strong anisotropic disorder which can be taken into account by anisotropic thermal vibrations (dynamic model) or by partially occupied split positions (static model). First we focus on the top-layer Ag atoms. The least-square refinement of the data sets was performed with the program PROMETHEUS, which was especially designed for the refinement of anharmonic thermal parameters [20]. The importance of anharmonic contributions to the thermal vibrations was demonstrated previously for Cs adsorbed on Cu(001), which forms a quasihexagonal monolayer [21].

Generally, without temperature-dependent data, it is not possible to decide whether the disorder is dynamic or static in nature. Therefore, in addition to a large data set taken at 210 K, several smaller data sets at 166, 170 and 313 K were recorded which allow refinement of the in-plane vibrations. The result for the top-layer Ag atoms ($Ag_{(1)}$) is shown in Fig. 2, where the harmonic mean square displacements U^{11} parallel to [110] and U^{22} parallel to [1$\bar{1}$0] are plotted versus temperature. Two results are directly evident: (i) the linear dependency of the U^{ii} ($i = 1,2$) on the temperature indicates the dynamic nature of the Ag disorder. (ii) The dynamic disorder is distinctly anisotropic, as can be seen by the different slopes of U^{ii} as represented by the straight lines fitted through the datapoints and extrapolated through the origin (Fig. 2). Assuming harmonic vibrations, Debye temperatures of $\Theta_D^{11} = 31$ K and $\Theta_D^{22} = 80$ K are derived using the relation $U^{ii} = 3\hbar T/(mk\Theta_D)$, where m and k represent the mass of the Ag atoms and Boltzmann's constant, respectively [22]. Taking account of the anisotropy of the $Ag_{(1)}$ vibrations was a prerequisite for obtaining a good agreement between observed and calculated structure-factor amplitudes ($|F_{obs}|$,$|F_{calc}|$). For all data sets the differences were 5–10%.

For the highest temperature (313 K) we observe one significant deviation from the linear dependence of U^{22} on the temperature, where the vibration amplitude becomes almost isotropic ($U^{11} \approx U^{22}$). This isotropization of the disorder might be attributed to the onset of the breakdown of the superstructure, which was also observed in the Cs/Cu(001) system [21]. For the K atoms we also observe significant anisotropy of the disorder, which could not be analyzed in such detail since the contribution of the weakly scattering K atoms to the total amplitude is small, especially at this low coverage.

In order to analyze the structure in three dimensions and to quantify the disorder in more detail, a large data set was taken at 210 K. The results

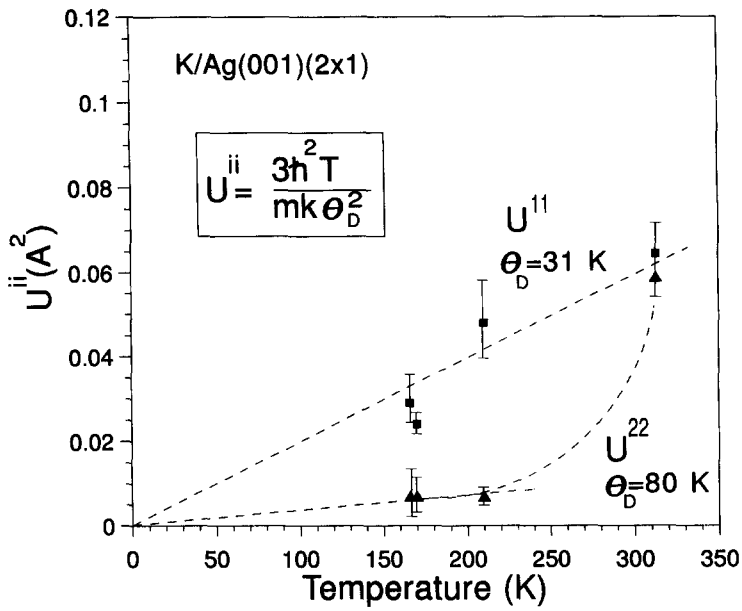

Fig. 2. Plot of the (in-plane) harmonic mean squared vibration amplitudes of the top-layer Ag atom ($Ag_{(1)}$) along [110] (U^{11}) and [1$\bar{1}$0] (U^{22}) as a function of temperature. The dashed lines extrapolated through the origin indicate Debye-like behaviour. From the slopes of the lines, Debye temperatures (Θ_D) of 31 and 80 K are derived.

are summarized in Table 1. Two refinements are compared, the first allowing only for harmonic $Ag_{(1)}$ vibrations ("harmonic"), the second additionally taking account of anharmonic contributions ("anharmonic"). For the K atoms and second-layer Ag atoms (Ag_2), only harmonic vibrations were considered. First, we discuss the harmonic refinement.

The comparison of U^{ii} ($i=1,2,3$) derived for the top-layer Ag atom indicates that the vibration amplitude normal to the sample surface ($U^{33}=0.117(21)$ Å^2) is significantly larger than the inplane vibrations ($U^{11}=0.048(9)$ Å^2, $U^{22}=0.007(2)$ Å^2). In their LEED experiments on the unreconstructed Ag(001) surface, Morabito et al. [23] derived a surface Debye temperature of 104 K which did not show a notable anisotropy. In this context our results point directly to the sensitivity of the thermal disorder to the "openness" of the surface structure. Along the densely packed Ag chain, where the local (2 × 1) structure is most similar to the structure of the unreconstructed surface, we derive $\Theta^{22}=80$ K, which is comparable with the LEED result. In contrast, the openness of the MR structure along [110] leads to considerably larger vibration amplitudes normal to the chain direction, as expressed by $\Theta^{11}=31$ K. Moreover, a vibration amplitude normal to the sample surface larger than that parallel to it has already been observed for clean metal surfaces such as W(100) [24], and can be understood by its intrinsic anisotropy. However, this is not a general rule and depends on the local structure and on the surface bonding. Recent LEED experiments by Löffler et al. [25] on K adsorption on Ni(001) have shown the in-plane K vibrations to be larger than the normal vibrations. For K vibrations within the MR adsorption site we observe more disorder along the grooves than perpendicular to them or normal to the sample surface. Apart from the dynamics, the structure parameters can be summarized as follows (see also Table 1). The K–Ag bond lengths are in the range 3.40–3.50 Å, corresponding to an effective K radius of about 2.0 Å if a metallic Ag radius of 1.44 Å is assumed. This agrees well with a number of investigations on K-adsorption on metal surfaces (for an overview, see Ref. [26]). For the harmonic

Table 1
Structure parameters derived for the K/Ag(001)-(2×1) reconstruction allowing for harmonic and anharmonic displacement factors of the top-layer Ag atoms; the atoms are labeled according to Fig. 2; parameters kept fixed during the refinement are asterisked; the terms "mean" and "mode" refer to the different definitions of the atomic position for $Ag_{(1)}$ in the case of anharmonic refinement.

	Harmonic	Anharmonic
K occupancy factor	0.249±0.067	0.397±0.062
d_K (Å)	1.34±0.16	1.17±0.05 (mean)
K–Ag_1 (Å)	3.50±0.15	3.43±0.05 (mean)
K–Ag_2 (Å)	3.43±0.19	3.44±0.05 (mean)
δ_x (Å)	0.03±0.01	0.04±0.05 (mean)
$Ag_{(1)}$–$Ag_{(2)}$ (Å)	2.72±0.10	2.86±0.05 (mean)
d_{12} (Å)	1.78±0.10	1.98±0.05 (mean)
d_{12} (Å)	1.78±0.10	1.96±0.05 (mean)
Atomic displacement parameters		
$Ag_{(1)}$		
U^{11} (Å^2)	0.048±0.009	0.048±0.009
U^{22} (Å^2)	0.007±0.002	0.014±0.002
U^{33} (Å^2)	0.117±0.021	0.508±0.045
C^{113} (×10^3)	—	0.783±0.269
C^{333} (×10^3)	—	−20.950±3.560
D^{1111} (×10^4)	—	0.073±0.034
D^{1122} (×10^4)	—	0.032±0.018
D^{1133} (×10^4)	—	1.362±0.387
$Ag_{(2)}$		
B (Å^2)	0.63±0.36	1.84±0.32
K		
U^{11} (Å^2)	0.020*	0.021±0.019
U^{22} (Å^2)	0.216±0.200	0.392±0.211
U^{33} (Å^2)	0.020*	0.020*
Agreement parameters		
R_w (weighted R)	0.058	0.029
R_u (unweighted R)	0.091	0.047
GOF	1.670	0.938

refinement we derive an Ag interlayer spacing d_{12} of 1.78±0.10 Å. This corresponds to a contraction of 12.7% compared to the bulk Ag interlayer spacing (2.043 Å). Finally, for the K occupancy we obtain 0.249(67) for the harmonic refinement and 0.397(67) for the anharmonic refinement, corresponding to a K coverage of 0.12 and 0.20 ML. Although there is considerable variation in the refinement, which can be attributed to the low K-contribution to the whole scattering amplitude, both results are reasonably close to the reported value of about 0.15 ML for the (2×1) superstructure to form.

Although the structural parameters appear quite reasonable, the goodness of fit parameter (GOF) [16] is only 1.67, indicating that there is still room for improvement. Since the consideration of a third Ag layer did not lead to an improvement of the fit and to reasonable results, we tried a structure refinement including anharmonic contributions to the $Ag_{(1)}$ thermal disorder. This seems especially justified in view of the large vibration amplitudes, which indicate a very weak surface lattice. Anharmonic effects were not found to be significant for K and the second-layer Ag atom.

The anharmonicity is taken into account by the Gram–Charlier (GC) series expansion of the harmonic (Gaussian) probability density function $PDF_H(\boldsymbol{u})$ [12,27,28],

$$PDF_{GC}(\boldsymbol{u}) = PDF_H(\boldsymbol{u})\left[1+\frac{1}{3!}c^{klm}H_{klm}(\boldsymbol{u}) + \frac{1}{4!}c^{klmn}H_{klmn}(\boldsymbol{u})+\ldots\right], \quad (1)$$

where $\boldsymbol{u}$ represents the displacement vector from the minimum potential position $\boldsymbol{u}_0$ (mode position, see below). The multidimensional Hermite polynomials $H_{klmn\ldots r}(\boldsymbol{u})$ are the rth-order derivatives of $PDF_H(\boldsymbol{u})$ with respect to $\boldsymbol{u}$. The Fourier transform of Eq. (1) leads to a generalized temperature factor $T_{GC}(\boldsymbol{h})$, which is given by a series expansion of the harmonic temperature factor $T_H(\boldsymbol{h})$

$$T_{GC}(\boldsymbol{h}) = T_H(\boldsymbol{h})\left[1+\frac{(2\pi i)^3}{3!}h_k h_l h_m C^{klm} + \frac{(2\pi)^4}{4!}h_k h_l h_m h_n D^{klmn}+\ldots\right]. \quad (2)$$

Using this equation, a generalized expression for the structure factor is obtained

$$F_{GC}(\boldsymbol{h}) = \sum_j f_j e^{i2\pi h_k x_j^k - 8\pi^2 U_j^{kl} h^k h^l} \times\left[1 - i\frac{4}{3}\pi^3 h_k h_l h_m C_j^{klm} + \frac{2}{3} \times \pi^4 h_k h_l h_m h_n D_j^{klmn} - \ldots\right], \quad (3)$$

where h_j corresponds to the components of the reflection indices ($j=1,2,3$), and the sum convention has to be applied. The anharmonic corrections for the jth atom in the structure-factor equation are given up to fourth order by the (dimensionless) tensor coefficients C_j^{klm} and D_j^{klmn}. The first- and second-order terms of the series expansion are set to zero, which means that the average and the standard deviation of the harmonic part include the anharmonic first- and second-order contributions.

Symmetry restrictions considerably reduce the number of anharmonic refinement parameters. Due to the high 2mm site symmetry the number of higher-order coefficients is considerably reduced, which allows analysis of the anharmonicity as has been done in Ref. [21]. However, in this case we deal with a three-dimensional problem introducing third-order coefficients and some additional fourth-order coefficients. However, the number of independent reflections (39) is much larger in this case, allowing the unambigous refinement of the anharmonicity coefficients and the structural parameters as expressed by the GOF parameter [16].

Out of a maximum of ten third-order and 15 fourth-order coefficients in the general case, only three third-order (C^{333}, C^{113} and C^{223}) and six fourth-order coefficients (D^{1111}, D^{2222}, D^{3333}, D^{1122}, D^{1133} and D^{2233}) remain as fitting parameters for $Ag_{(1)}$. Furthermore, four coefficients were rejected as insignificant and set to zero as their standard deviations were 60–100%. Table 1 summarizes the results. The refinement including anharmonicity improved the fit dramatically. The standard deviations of the refined anharmonic coefficients are generally below 50% (for C^{333} it is only 17%), and thus the refinement results can be considered to be highly significant. In addition it should be emphasized that the error bars for the structural parameters decrease with consideration of the anharmonicity as compared to the harmonic refinement. This is in accordance with the low correlation of the $Ag_{(1)}$ positional parameters with the higher-order coefficients, the maximum being 0.46.

In order to additionally verify the results in view of the limited data set, we also tried fits with a reduced number of reflections. It turned out that both the structural as well as the anharmonicity parameters (and with them the calculated effective one-particle potentials, see below) are still reproduced within the error bars even if only half of the reflections along the rods are included. In general, deviations were only observed if in addition more than 4–5 in-plane reflections are excluded from the data set. However, even in this case, the most significant coefficient (C^{333}) does not show deviations larger than the error bar from the value obtained with the full data set.

Finally, it should be added that both the structural parameters as well as the vibration parameters of the first-layer Ag atoms might be different depending on whether or not the Ag atom is neighboured by K. In principle this could be taken into account by two partially occupied $Ag_{(1)}$ atoms (e.g. occupation factors 0.30 and 0.70, corresponding to the fraction of $Ag_{(1)}$ atoms which have K neighbours or not, respectively) and independent refinement of all parameters. In the present case this attempt failed because of the limited data set and (more importantly) due to the high correlation between the parameters of the two Ag atoms. Consequently, in the refinement discussed here we obtain an average of the (probably) different $Ag_{(1)}$ structure parameters which, however, can be suspected to correspond mostly to those Ag atoms not neighboured by K atoms.

A direct representation of the temperature factor is possible by calculating the PDFs for both the harmonic and the anharmonic refinements. This is shown in Fig. 3, where the PDFs of the first- and second-layer Ag atoms are shown in a plane that is spanned by vectors parallel to [100] and [001]. The section of the plane with the (001) surface is indicated by the dashed line in the inset of Fig. 3. For $Ag_{(1)}$ a significant deviation of the PDF from the (harmonic) ellipsoidal shape along [001] is evident, and can be attributed to the large magnitude of the C^{333} coefficient.

It should be noted that whenever anharmonic terms are involved in the calculation of the temperature factor and the effective one-particle potentials (OPPs) [12,20,27], a distinction has to be made between different expressions for the atomic positions. The mean position is the refined first-order

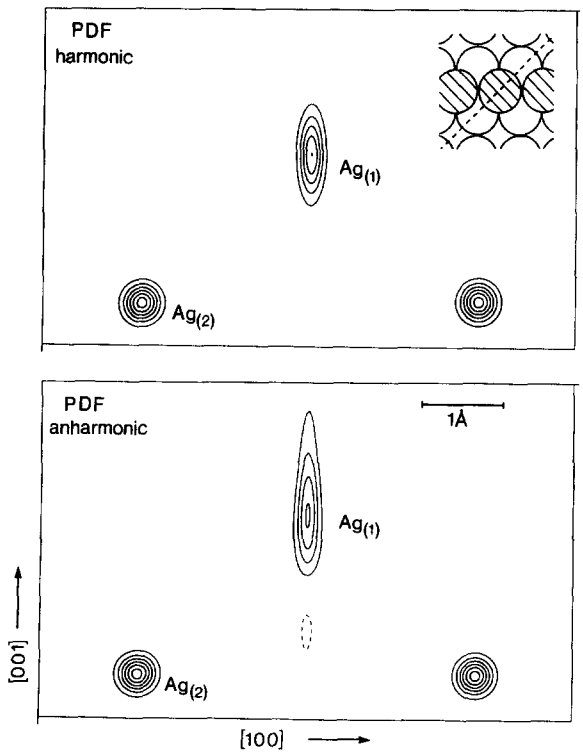

Fig. 3. Probability density function $Ag_{(1)}$ and $Ag_{(2)}$ for the harmonic and anharmonic refinement in a plane defined by vectors parallel to [100] and [001]. The section of the plane with the (001) surface is given by the dashed line in the inset.

term x_j^k in the series expansion (Eq. (3)). The so-called "mode position" is given by the minimum of the OPP, where the OPP is given by $V(\boldsymbol{u}) = -kT \ln[\mathrm{PDF}(\boldsymbol{u})/\mathrm{PDF}(\boldsymbol{u}_0)]$. In other words, the mode position corresponds to $\boldsymbol{u} = \boldsymbol{u}_0$, the maximum of the PDF. The physically most important positional parameter is the equilibrium position $M(\boldsymbol{u})$, which is the true mean position of an atom at a given temperature. The equilibrium position $M(\boldsymbol{u})$ can be evaluated using the calculated OPP by

$$\int \boldsymbol{u}\, \mathrm{e}^{-V(\boldsymbol{u})/kT}\, \mathrm{d}\boldsymbol{u} \Big/ \int \mathrm{e}^{-V(\boldsymbol{u})/kT}\, \mathrm{d}\boldsymbol{u},$$

corresponding to the quantum mechanical expectation value of $\boldsymbol{u}$. Only in the harmonic case are the mean, mode and equilibrium positions identical. If only even-order terms of the general structure factor (Eq. (3)) are involved, at least the mean and the equilibrium positions are identical. In the presence of odd-order modifications (as discussed here) the mean, mode and equilibrium positions may differ.

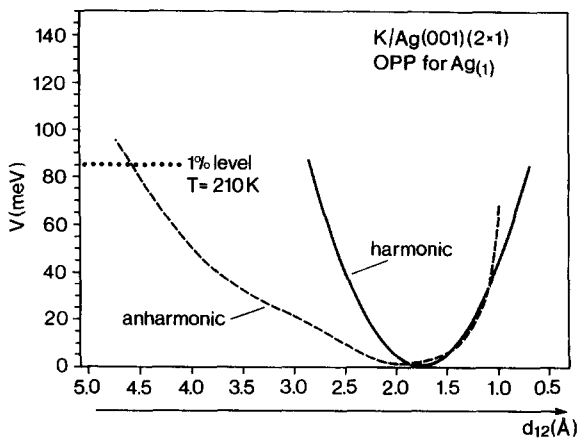

Fig. 4. Effective one-particle potentials for the $Ag_{(1)}$ vibration normal to the sample surface as derived on the basis of the PDFs for harmonic (solid line) and anharmonic (dashed line) refinement. The abscissa indicates the Ag interlayer spacing d_{12}, and the dashed line at about 85 meV represents the 1% occupation probability of the energy state at 210 K according to Bose–Einstein statistics.

The OPPs along [001] are shown in Fig. 4 for both the harmonic and the anharmonic refinement as solid and dashed lines, respectively. The abscissa refers to the interlayer distance d_{12}. Whereas the harmonic temperature factor is related to the parabolic potential, the anharmonic refinement leads to a potential that shows significant deviations from a parabola along both directions. There is a steeper increase of the potential at low distances which can be related to the "hard wall" repulsion between the neighboring Ag layers, but a slower increase at longer distances. The latter is the most important factor which contributes to the anharmonicity, as is also evident from the PDF in Fig. 3. In order to check the detailed physical significance of the refined potentials, the analysis of temperature-dependent data must lead to potentials that are independent of temperature. In the present case, high-quality temperature-dependent data are not available. Nevertheless, in order to discuss the basic features of the $Ag_{(1)}$ anharmonicity the consideration of the OPP appears justified, especially

in view of the high significance of the refined anharmonicity coefficients.

For interpretation of the potentials, the occupation of the energy states has to be taken into account. At low temperatures only a few atoms have a high energy, and therefore the potential is not well defined at points far away from the mode position. For a rough estimation of the occupation, the Bose–Einstein distribution can be considered; although it is strictly valid only for a parabolic potential and for flat potentials, it leads to an overestimation. In Fig. 4 the dotted horizontal line at about 85 meV indicates the energy level at which an occupation probability of 0.01 is calculated for $T=210$ K. Thus at this temperature the major fraction of the atoms is close to the potential minimum. Based on the results discussed so far we can analyze the different positional parameters (mean, mode and equilibrium positions) for the $Ag_{(1)}$ atom.

In the anharmonic refinement the Ag interlayer spacing is contracted by only 3.2% ($d_{12}=1.98\pm0.05$ Å) relative to the bulk interlayer spacing if we refer to the mean position of $Ag_{(1)}$. Nearly the same result is obtained if the distances are referred to the $Ag_{(1)}$ mode position ($d_{12}=1.96\pm0.05$ Å). In the case of the anharmonic refinement, the interlayer contraction is therefore smaller than in the harmonic case, where the contraction is derived to be 12.7%. Due to the pronounced deviation from a parabolic potential at large distances from the surface, a reduced interlayer contraction can also be expected if the equilibrium position $M(\boldsymbol{u})$ of $Ag_{(1)}$ is considered. In order to obtain an estimation for $M(\boldsymbol{u})$ we calculated the expectation value

$$\int \boldsymbol{u}\, e^{-V(\boldsymbol{u})/kT}\, d\boldsymbol{u} \Big/ \int e^{-V(\boldsymbol{u})/kT}\, d\boldsymbol{u},$$

numerically. For the anharmonic case we obtain $d_{12}=2.10$ Å, which could be interpreted as an interlayer spacing which is expanded, or at least which is not contracted within an error bar of about 3% if we keep in mind that the result for $M(\boldsymbol{u})$ is based on a number of approximations. In summary, this structure analysis, taking account of anharmonic contributions to the thermal disorder, demonstrates the influence of the correct treatment of the thermal disorder on the correct determination of distance.

4. Summary

We have presented a surface XRD analysis of the K/Ag(001)-(2 × 1) reconstruction. The structure is an MR geometry in which every other row of Ag atoms along [1$\bar{1}$0] is missing and the K atoms reside within the large grooves of the MR structure, coordinated by six Ag atoms at a distance of 3.44(5) Å. Using this result an effective K radius of about 2.0 Å is derived, which is in good agreement with a number of different studies of K adsorption on metal surfaces. For both the K atoms and the top-layer Ag atoms, pronounced anisotropic thermal vibrations were found. Whereas the K vibrations are most pronounced parallel to the MR direction, the Ag vibrations are stronger perpendicular to the MR direction, and especially normal to the sample surface. The consideration of anharmonic temperature parameters is found to be of crucial importance for the proper description of the structure. The refinement of anharmonic contributions to the temperature factor was performed using the Gram–Charlier series, which is well known in bulk crystallography. Including odd-order tensor parameters into the refinement makes new definitions of the positional parameters (mean, mode and equilibrium positions) necessary. In the present case we have shown that the first Ag interlayer spacing (d_{12}) is determined too compressed relative to the bulk spacing (13.7%) if only harmonic terms are included in the refinement. On the other hand, including anharmonicity the compression turns out to be at most 3.2%.

Acknowledgements

One of us (H.L.M.) would like to thank AT&T for providing access to beamline X16A and their hospitality during his visit in Brookhaven. The support of the Bundesministerium für Wissenschaft und Forschung under Grant #05464IAB8 is grate-

fully acknowledged. Work at the NSLS is supported by the US Department of Energy under DE-AC 012-76CH0016. Additional support came from the University of Illinois Materials Research Laboratory under grant DEFG02-96ER45439.

References

[1] B.E. Hayden, K.C. Prince, P.J. Davies, G. Paolucci and A.M. Bradshaw, Solid State Commun. 48 (1983) 325.
[2] C.J. Barnes, M.Q. Ding, M. Lindroos, R.D. Diehl and D. King, Surf. Sci. 162 (1985) 59.
[3] S.M. Francis and N.V. Richardson, Surf. Sci. 152/153 (1985) 63.
[4] R.J. Behm, G. Ertl, D.K. Flynn, K.D. Jamison and D.A. Thiel, Phys. Rev. B 36 (1987) 9267.
[5] R. Schuster, P.J. Eng and I.K. Robinson, Surf. Sci. 326 (1995) L477.
[6] R. Schuster and I.K. Robinson, Phys. Rev. Lett. 76 (1996) 1671.
[7] K.W. Jacobson and J.K. Nørskov, Phys. Rev. Lett. 60 (1988) 2496.
[8] M. Okada, H. Tochihara and Y. Murata, Phys. Rev. B 43 (1991) 1411.
[9] M. Okada, H. Tochihara and Y. Murata, Surf. Sci. 245 (1991) 380.
[10] S. Mizuno, H. Tochihara and T. Kawamura, Surf. Sci. 292 (1993) L811.
[11] O.B. Christensen and K.W. Jacobson, Phys. Rev. B 45 (1992) 6893.
[12] W.F. Kuhs, Acta Cryst. A 48 (1992) 80.
[13] L. Wenzel, D. Arvanitis, H. Rabus, T. Lederer and K. Baberschke, Phys. Rev. Lett. 64 (1990) 1765.
[14] P. Zeppenfeld, K. Kern, R. David and G. Comsa, Phys. Rev. Lett. 62 (1989) 63.
[15] M.A. van Hove, W.H. Weinberg and C.-M. Chan, Low Energy Electron Diffraction, Vol. 6 of Springer Series in Surface Sciences (Springer, Berlin, 1986).
[16] I.K. Robinson, in: Handbook of Synchrotron Radiation, Vol. 3, Eds. G.S. Brown and D.E. Moncton (Elsevier, Amsterdam, 1991).
[17] P.H. Fuoss and I.K. Robinson, Nucl. Instrum. Methods 222 (1984) 171.
[18] We use a sample setting corresponding to a primitive (1×1) surface unit cell, therefore the *a*-, *b*- and *c*-axes of the surface unit cell are parallel to [110], [1$\bar{1}$0] and [001] of the fcc unit cell.
[19] H.L. Meyerheim, S. Pflanz, R. Schuster and I.K. Robinson, Physica B 221 (1996) 134.
[20] U.H. Zucker, E. Perenthaler, W.F. Kuhs, R. Bachmann and H. Schulz J. Appl. Cryst. 16 (1983) 358.
[21] H.L. Meyerheim, W. Moritz, H. Schulz, P.J. Eng and I.K. Robinson, Surf. Sci. 331–333 (1995) 1422.
[22] It should be noted that it is not strictly correct to refer to an anisotropic Debye temperature, since the Debye theory is based on the isotropy of the phonon group velocity. Nevertheless, in order to emphasize the anisotropy of thermal vibrations, anisotropic Debye temperatures are often used formally.
[23] J.M. Morabito, R.F. Steiger and G.A. Somorjai, Phys. Rev. 179 (1969) 638.
[24] L. Dobrzynski and P. Masri, J. Phys. Chem. Solids 33 (1972) 1603.
[25] U. Löffler, U. Muschiol, P. Bayer, K. Heinz, V. Fritsche and J.B. Pendry, Surf. Sci. 331–333 (1995) 1435.
[26] R.D. Diehl and R. McGrath, Surf. Rev. Lett 2 (1995) 387.
[27] U.H. Zucker and H. Schulz, Acta Cryst. A 38 (1982) 563.
[28] C.K. Johnson and H.A. Levy, in: The International Tables for X-Ray Crystallography, Vol. IV (Kynoch Press, Birmingham, 1974).